Hindawi
Journal of Advanced Transportation
Volume 2023, Article ID 4866326, 18 pages
https://doi.org/10.1155/2023/4866326

Research Article

Boundary Guidance Strategy and Method for Urban Traffic Congestion Region Management in Internet of Vehicles Environment

Chuanxiang Ren,[1] **Zhen Wang**,[1] **Changchang Yin**,[2] **Hui Xu**,[1] **Li Wang**,[1] **Luyao Guo**,[1] **and Juntao Li**[3]

[1]*College of Transportation, Shandong University of Science and Technology, Qingdao 266590, China*
[2]*College of Electrical Engineering and Automation, Shandong University of Science and Technology, Qingdao 266590, China*
[3]*School of Information, Beijing Wuzi University, Beijing 101149, China*

Correspondence should be addressed to Changchang Yin; ycc2009@sdust.edu.cn

Received 15 January 2023; Revised 18 April 2023; Accepted 24 April 2023; Published 4 May 2023

Academic Editor: Socrates Basbas

Accelerated urbanization has increased regional traffic congestion. To alleviate traffic congestion in a homogeneous road network, combined with the advantage of real-time traffic information obtained by the Internet of Vehicles (IoVs), a boundary guidance strategy for traffic congestion region is proposed. The strategy considers the optimal operation state of traffic congestion region and is divided into two categories according to different destinations of traffic demands. Meanwhile, a method for the boundary guidance strategy is presented in which the macroscopic fundamental diagram (MFD) is used to determine the optimal accumulation, a traffic flow equilibrium model is established to calculate the real-time accumulation, and a fuzzy adaptive PID control algorithm is designed to calculate the optimal traffic inflow of the traffic congestion region. Furthermore, an example is selected for simulation. The results show that the boundary guidance strategy can effectively improve the operational state of the road network and alleviate traffic congestion. Finally, the influence of connected vehicle penetration rate on the strategy is discussed. The simulation results show that the strategy can improve the operation state of the road network under mixed traffic flow, and the higher the penetration rate, the more significant its effect on alleviating traffic congestion.

1. Introduction

With the development of the economy and the accelerated urbanization of society, the number of vehicle ownership is increasing, and urban traffic congestion is becoming a more serious problem. In order to solve the problem of urban traffic congestion, intelligent transportation systems have been developed rapidly [1]. Among them, the traffic guidance subsystem, as an important part of the intelligent transportation system, can guide vehicles to avoid congested links or regions. All with the goal to alleviate the traffic congestion. Thus, the traffic guidance subsystem has become an important means to solve the urban traffic congestion problem [2, 3]. Due to the different traffic demands, the traffic flow within the traffic regions that make up the urban road network has its own characteristics, and there is often a spatial heterogeneity characteristic, which makes traffic regions often experience serious congestion [4]. How to use traffic guidance to avoid serious congestion, reduce the duration of congestion, and improve the traffic efficiency has become a hot topic for researchers in the field of traffic engineering.

Urban traffic guidance is mainly conducted through the release of information by variable message signs (VMS), traffic broadcasts, and vehicle terminal [5]. VMS and traffic broadcast mainly target groups of vehicles for traffic guidance, which can quickly alleviate traffic congestion in links or regions. However, VMS have problems such as

insufficient dynamics and coordination and content limitations of information [6]. Traffic broadcast has the problems of signal timeliness and instability [7]. The vehicle terminal, which can release diversified information, has become a carrier for more effective traffic guidance and is gradually being applied in urban traffic guidance [8]. Furthermore, the development of Internet of Vehicles (IoVs) in recent years has provided new prospects for improving the effect of urban traffic guidance. Traffic guidance based on IoVs has attracted the attention of scholars in the field of transportation, such as the use of IoVs to achieve the optimal system or optimal user route guidance [9, 10]. Especially, the widespread application of roadside units (RSU) in urban traffic management [11, 12], which can exchange information with connected vehicles in real time, makes it easier and faster to obtain the information of vehicles entering from the boundary of the region [13]. This provides a powerful support for more accurate guidance in urban traffic congestion regions. Traffic guidance based on IoVs has received attention from scholars and achieved some results [3, 14–16]. However, existing traffic guidance methods based on IoVs do not consider the optimal inflow of the congestion region and do not differentiate the destinations of traffic demand entering the congestion region. In addition, the influence of connected vehicle penetration on traffic guidance should also be further studied. Based on this, a boundary guidance strategy is proposed to achieve the optimal management of traffic demand, and simulation is conducted with the obtained results discussed to prove the effectiveness of the proposed approach.

The contributions of this paper are mainly related to the following four aspects:

(1) Based on the real-time traffic information from IoVs, a boundary guidance strategy for congestion region is proposed, which classifies traffic demands according to destinations and conducts guidance for traffic demands whose destination is a non-congestion region to maintain the optimal operation state of the region.

(2) A method for guidance is designed, including the use of a macroscopic fundamental diagram (MFD) to determine the optimal accumulation, the establishment of a traffic flow equilibrium model for the traffic congestion region under an optimal operation state to calculate real-time accumulation, and the design of a fuzzy adaptive PID control algorithm to calculate the optimal inflow.

(3) The boundary guidance strategy is simulated and verified, and the results show that it can effectively improve the operation state of a road network and alleviate traffic congestion.

(4) The influence of connected vehicle penetration rate on the boundary guidance strategy is discussed. The simulation results under different penetration rates show that the boundary guidance strategy can improve the operation state of the regional road network under mixed traffic flow, and the higher the penetration rate, the more significant its effect on alleviating traffic congestion.

The rest of the paper is organized as follows: Section 2 presents the current status of research related to traffic guidance. Section 3 proposes the boundary guidance strategy for the traffic congestion region. In Section 4, the method for the boundary guidance strategy is presented. Section 5 simulates and validates the proposed boundary guidance strategy and method with an example region. Section 6 discusses the influence of connected vehicle permeation rate on the boundary guidance strategy. Finally, the conclusion and outlook are given in Section 7.

2. Literature Review

The most typical way of providing urban traffic guidance is based on VMS, and many scholars have conducted a series of studies on traffic guidance based on VMS. Zhong et al. [17] studied the effect of VMS location on drivers' compliance behavior and found that the further the VMS is from the downstream intersection, the better the guidance effect. Li et al. [18] studied the effect of VMS layout on traffic guidance effect using a genetic algorithm, and the results showed that reasonable VMS settings can effectively alleviate traffic congestion. Jindahra and Choocharukul [19] studied the influence of VMS content on a driver's route choice using driver's preference data. The results showed that different types of information causes different levels of route switching. Zhao et al. [20] investigated the interrelationship between weather conditions and VMS format, and the results showed that drivers prefer graphic or single-line information in foggy weather. AlKheder et al. [21] studied the impact of VMS information on drivers' lane-changing behaviors. The results show that when the VMS displays multiple messages, it affects the driver's decision to change lanes. Zhao et al. [22] analyzed a dataset of preference questionnaires and found that accident information had a greater impact on driver compliance behavior than information about road construction and congestion. Shen and Yang [23] studied the impact of different congestion messages on drivers and found that VMS had the greatest impact on drivers in heavy traffic congestion conditions. Roca et al. [24] evaluated the difficulty of accessing VMS information for dyslexic patients and found that they were more receptive to information from a pictogram VMS. Tejero et al. [25] studied the effects of different forms of VMS on drivers and found audio versions could improve the driving performance.

However, the guidance information in VMS is open to all travelers and cannot be used to conduct dynamic route planning based on the travel demand of the guidance target. In order to further improve the effectiveness of traffic guidance, some advanced methods have been proposed by scholars. Wang et al. [26] proposed an optimal information feedback strategy, which introduces congestion coefficients and achieves dynamic route guidance using real-time information feedback. Lin et al. [27] proposed a real-time route guidance strategy with dynamic route decisions. The

strategy introduces trust probability to predict traffic conditions and dynamically determine optimal routes. Zhao and Zhang [28] proposed a dynamic route guidance method based on a hidden Markov model to improve the real-time and accuracy of traffic guidance information. Ding et al. [29] proposed a combined route guidance and perimeter control method with the objective of minimizing network delay. Simulation results show that the method can reduce congestion in subregions. Yildirimoglu et al. [30] proposed a hierarchical traffic management system. Two mechanisms, route guidance and route assignment, are designed to provide subregional routes for vehicles to alleviate network congestion. Liu et al. [31] proposed a route evacuation guidance strategy by combining route guidance with perimeter control. The strategy effectively solves the flow distribution among regions and the route selection of travelers. Chen et al. [32] proposed a feedback strategy, which uses floating vehicle information to estimate nonfloating vehicle information and calculates the guidance index. Wei and Yang [33] proposed a two-level route guidance method for urban road networks based on MFD. The method solves the system-optimal and user-optimal problems at the subregion level. Cui et al. [34] explored the impact of different guidance strategies on traffic. Simulation results show that route guidance strategies based on average speed and congestion factor can improve the operational efficiency of the network. Wen et al. [35] proposed a route guidance algorithm based on hierarchical state–action–reward–state–action (SARSA) learning. Simulation results show that the method can improve the efficiency of the route guidance system on a large-scale road network. Tang et al. [36] proposed a route guidance method based on multiintelligent reinforcement learning. The method alleviates traffic congestion in a variety of traffic situations.

With the rapid development and application of IoVs, scholars have gradually applied them to traffic guidance and achieved some results. Amer et al. [37] proposed a route calculation method based on IoVs communication system. The method provides different route decisions according to the target to meet the driver's navigation needs. El-Sayed et al. [38] proposed a histogram-based route guidance algorithm, which is able to select the shortest route between the origin and destination. The experimental results show that the algorithm can solve the urban congestion problem. Lin et al. [39] proposed a social vehicle route selection algorithm, which uses a game evolution approach to calculate the optimal route. Sun et al. [40] proposed a collaborative optimization model of dynamic traffic control and guidance based on IoVs to improve the integrated effect of urban traffic systems and urban traffic guidance systems. Dow et al. [41] proposed an adaptive ITS service system, which generates a weighted road network and provides guidance and notification services based on IoVs. Nie et al. [42] proposed an automatic route guidance method based on vehicle self-organizing networks. Simulation results show that the method can improve the average vehicle speed as well as reduce delays. Bouyahia et al. [43] proposed a two-stage traffic resource scheduling strategy to solve the propagation of traffic congestion. Wang et al. [44] studied a real-time route planning model based on Vehicle to X (V2X) and proposed a route planning method considering traffic signal timing. The results show that the model can reduce the travel time. Khan et al. [45] proposed a road congestion detection and avoidance strategy based on IoVs. The simulation results show that the strategy can reduce the travel time. Zhang et al. [46] proposed an intelligent traffic model, which uses the predicted traffic flow and predicted waiting time to achieve signal control and route guidance. Nguyen and Jung [47] proposed the concept of exclusion pheromones for dispersed vehicle guidance through pheromones. Simulation results show that this method is effective in alleviating traffic congestion.

In summary, conventional route guidance strategies usually change the route from the user's perspective, and these routes usually avoid congestion regions and do not finely consider the traffic demand of the congestion regions. The traffic guidance methods based on IoVs improve the effectiveness of route guidance. However, they also ignore the optimal inflow of the congestion region and do not differentiate the destinations of traffic demand entering the congestion region. In this paper, the optimal operation state of the traffic congestion region is taken as the control objective, the optimal inflow of the congestion region and the destinations of the traffic demand are considered, and the congestion region boundary guidance strategy is proposed to achieve the optimal management of traffic demand and alleviate the traffic congestion.

3. Boundary Guidance Strategy for the Traffic Congestion Region

The application of IoVs enables the tracking of the information of vehicles entering and leaving the traffic congestion region, such as speed, location, destination, etc., to be obtained in real time by RSUs at the border and its upstream intersections. The RSUs transmit the obtained vehicle information to the cloud platform which is the decision center. Through the analysis of this information, the cloud platform can obtain the traffic inflow, outflow, and the state of the traffic congestion region. And then, the traffic inflow can be guided at the upstream intersections to avoid the increase of congestion and maintain the optimal operation state of the traffic congestion region. The schematic diagram of the guidance of the traffic congestion region is shown in Figure 1.

In Figure 1, there are three traffic regions: traffic region I, traffic region II, and traffic region III. Among them, region I is assumed as the traffic congestion region, while traffic region II and traffic region III are both noncongestion regions. In addition, all the upstream intersections closest to the boundary of traffic region I are virtualized as intersection C. Some of the exit lanes at these intersections correspond to the entrance lanes that can enter the boundary of region I. All the boundary intersections of region I are virtualized as intersection D, and these intersections contain exit lanes that can leave the region I.

The traffic demands of region I obtained by the RSU at intersection C, labelled as $Q_d(t)$, where t denotes time.

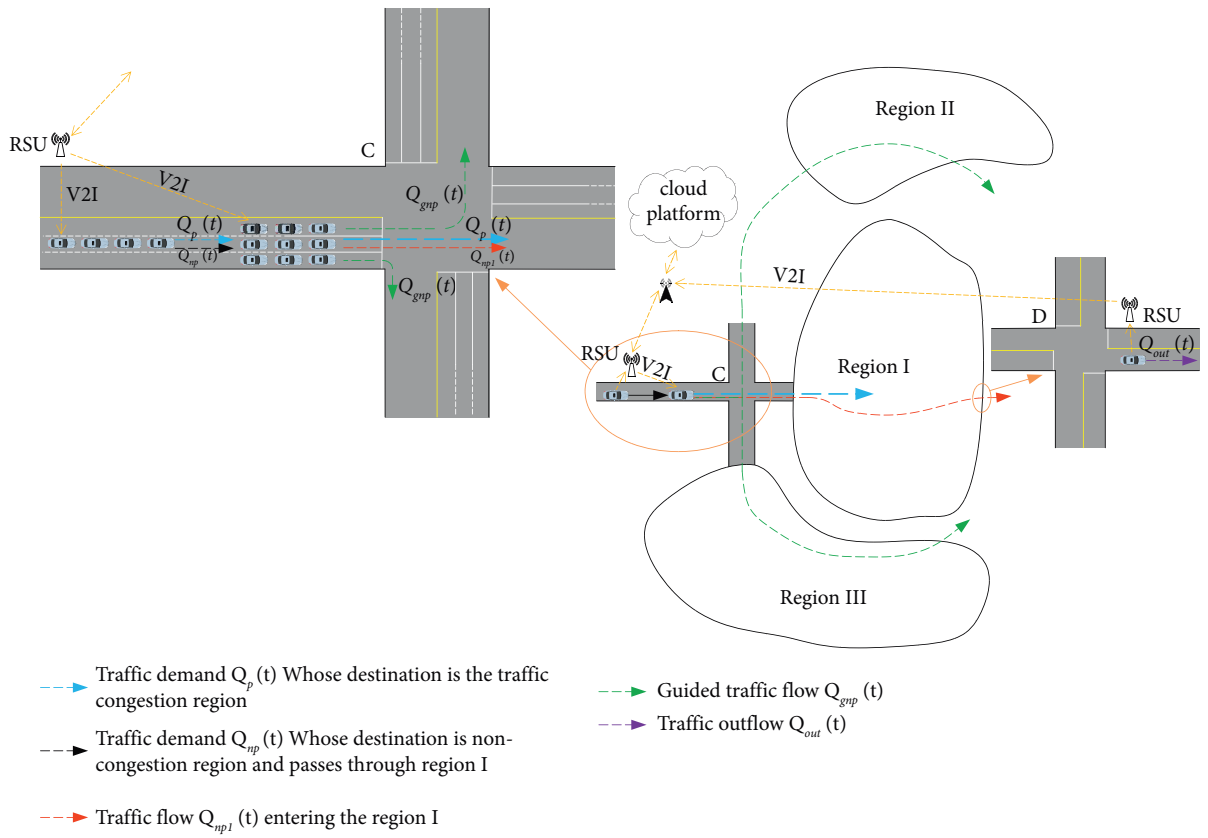

Figure 1: Schematic diagram of the boundary guidance.

According to the different destinations, the demand whose destination is the traffic congestion region is labelled as $Q_p(t)$, and the other whose destination is the noncongestion region and passes through region I is labelled as $Q_{np}(t)$. The traffic outflow obtained by the RSU at intersection D is labelled as $Q_{out}(t)$.

With the traffic inflow and outflow, the optimal accumulation is determined according to MFD theory, which is used as the guidance goal for the traffic congestion region.

When accumulation exceeds the value of optimal accumulation, the boundary guidance strategy takes effect. The fuzzy adaptive PID control algorithm is used to calculate the optimal traffic inflow, labeled as $Q_{op}(t)$.

If $Q_d(t) > Q_{op}(t)$, then the traffic demand $Q_{np}(t)$ in $Q_d(t)$ will be guided. The guided traffic demand will be divided into traffic flow entering region I, $Q_{np1}(t)$, and traffic flow entering the noncongestion region, $Q_{gnp}(t)$. The whole guidance process is shown in Figure 2, and the specific guidance strategy is as follows.

3.1. Boundary Guidance Strategy I (BGS I). When $Q_p(t) \le Q_{op}(t)$, boundary guidance strategy I is applicable. In this case, the traffic demand whose destination is the traffic congestion region is less, and more traffic demand is that whose destination is a noncongestion region. Thus, the traffic demand that needs to be guided can be expressed as follows:

$$\begin{aligned} Q_{np1}(t) &= Q_{op}(t) - Q_p(t), \\ Q_{gnp}(t) &= Q_{np}(t) - Q_{np1}(t). \end{aligned} \tag{1}$$

And the traffic inflow of the traffic congestion region, $Q_{in}(t)$, is equal to the optimal inflow, i.e., $Q_{in}(t) = Q_{op}(t)$.

3.2. Boundary Guidance Strategy II (BGS II). When $Q_p(t) > Q_{op}(t)$, boundary guidance strategy II is applicable. In this case, the traffic demand whose destination is the traffic congestion region is more, and the traffic demand whose destination is a noncongestion region is less. In order to maintain the operation state of the traffic congestion region as much as possible, it is necessary to guide all the demand whose destination is a noncongestion region, and $Q_{gnp}(t)$ can be obtained as follows:

$$Q_{gnp}(t) = Q_{np}(t). \tag{2}$$

Then the traffic inflow is equal to the traffic demand whose destination is the traffic congestion region, i.e., $Q_{in}(t) = Q_p(t)$.

4. Method

4.1. Macroscopic Fundamental Diagram. The implementation of the boundary guidance strategy needs to calculate the optimal accumulation. For this purpose, the MFD theory is utilized to describe the evolution of the traffic congestion

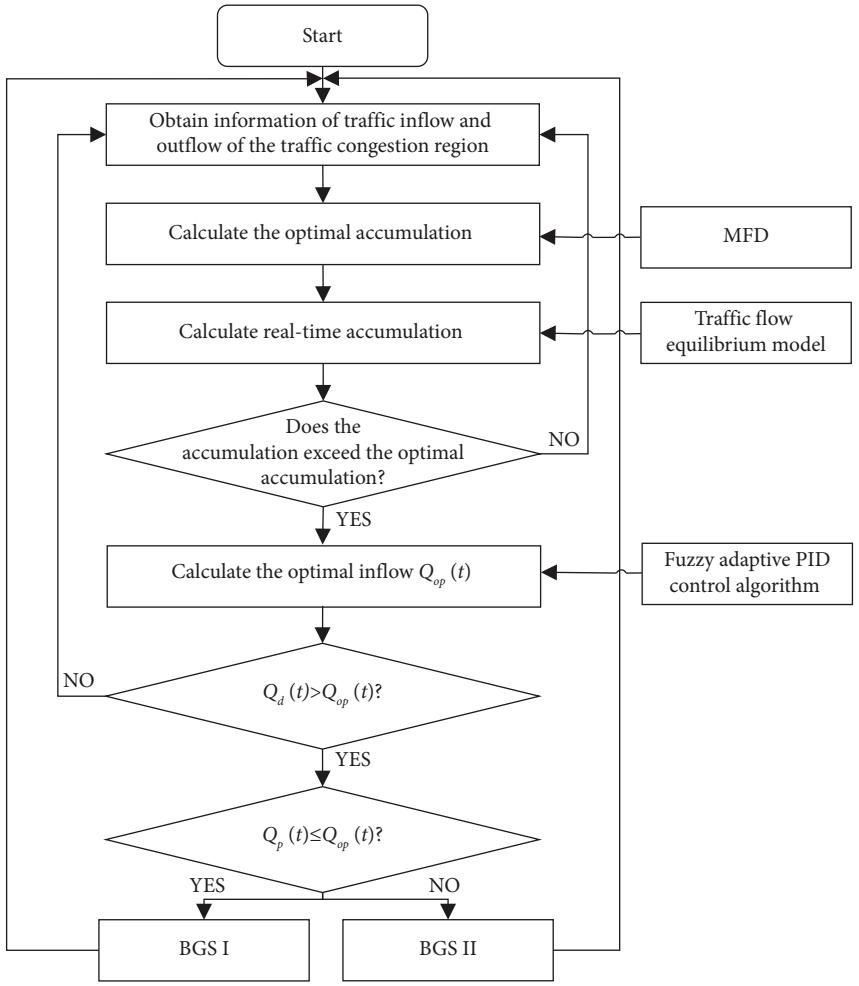

Figure 2: The process of guidance for the traffic congestion region.

region. MFD can describe the traffic operation state of a road network and is one of the effective ways to analyze urban traffic problems from a macro perspective [48, 49]. Usually, MFD is expressed by the relationship between the road network trip completion flow and the traffic accumulation, which is a nonnegative single-peaked curve [50], as shown in Figure 3. The horizontal axis is the traffic accumulation $N(t)$, and the vertical axis is the trip completion flow $G(N(t))$. The MFD curve is usually divided into three states. When the accumulation is from 0 to N_1, the MFD is in the ascending phase, indicating that the traffic flow is in the free flow state. When the accumulation belongs to N_1 to N_2, the trip completion flow fluctuates around $G_{\max}$, at which time the horizontal axis corresponds to the optimal accumulation, N_{op}, indicating that the traffic region is in the optimal operation state. When the accumulation exceeds N_2, the trip completion flow starts to decrease rapidly, indicating that the traffic region is in the oversaturation state.

According to the analysis of the MFD curve, when the accumulation exceeds the optimal accumulation, the traffic region tends to oversaturation state. Therefore, the optimal accumulation is used as the goal of the boundary guidance strategy, and the trip completion flow is represented by the traffic outflow. Moreover, the model for MFD can be generally expressed by a cubic polynomial [51], as follows:

$$G(N(t)) = a \bullet N^3(t) + b \bullet N^2(t) + c \bullet N(t), \tag{3}$$

where a, b, and c are the fitted parameters.

4.2. Traffic Flow Equilibrium Model. In order to achieve the goal of the optimal accumulation of boundary guidance strategies real-time accumulation of the traffic congestion region needs to be obtained. Whereas the accumulation is related to the traffic inflow and outflow, and the relationship can be obtained from the traffic flow equilibrium model. According to Aboudolas and Geroliminis [52, 53], a relatively stable MFD exists for each traffic region, and the presence of the MFD is independent of the OD distribution. To simplify the study, it is assumed that no traffic demand is generated within the traffic region. The traffic flow equilibrium model can be expressed as follows:

$$\frac{d(N(t))}{d(t)} = Q_{\text{in}}(t) - Q_{\text{out}}(t). \tag{4}$$

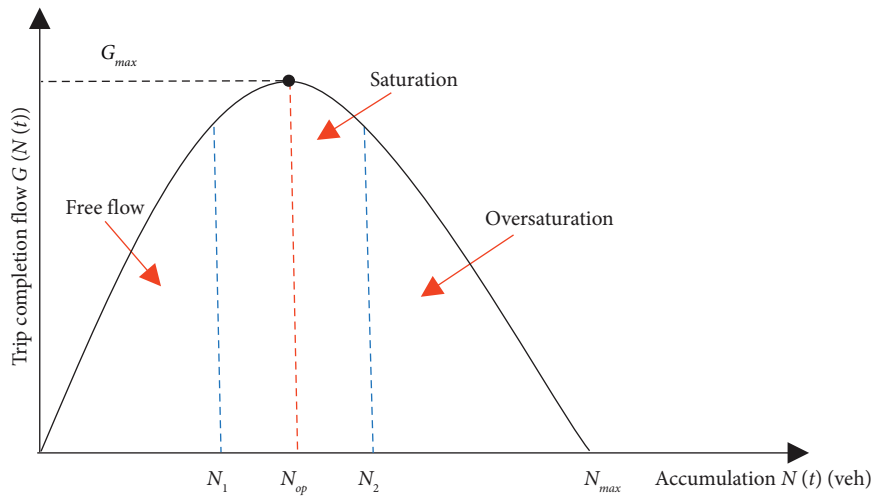

Figure 3: Macroscopic fundamental diagram.

Due to the traffic outflow is the trip completion flow, according to formula (3), it can be obtained as follows:

$$\frac{d(N(t))}{d(t)} = Q_{\text{in}}(t) - G(N(t)). \tag{5}$$

When the accumulation reaches the value of optimal accumulation, the trip completion flow is $G(N_{op})$, and let its corresponding inflow is Q_{op}^{in}, it can be obtained as follows:

$$Q_{\text{op}}^{\text{in}} = G\left(N_{\text{op}}\right). \tag{6}$$

Then the differences between the traffic inflow, trip completion flow, and accumulation and the optimal value corresponding to each quantity can be obtained as follows:

$$\Delta Q_{\text{in}}(t) = Q_{\text{in}}(t) - Q_{\text{op}}^{\text{in}}, \tag{7}$$

$$\Delta G(N(t)) = G(N(t)) - G\left(N_{\text{op}}\right), \tag{8}$$

$$\Delta N(t) = N(t) - N_{\text{op}}, \tag{9}$$

where $\Delta Q_{\text{in}}(t)$ is the difference between the inflow and $Q_{\text{op}}^{\text{in}}$, $\Delta G(N(t))$ is the difference between the trip completion flow and the trip completion flow corresponding to the optimal accumulation, $\Delta N(t)$ is the difference between the accumulation and the optimal accumulation

Substituting equations (6)–(9) into equation (5), the flow equilibrium model under the optimal operation state of the traffic congestion region can be obtained as follows:

$$\frac{d(\Delta N(t))}{d(t)} = \Delta Q_{\text{in}}(t) - \Delta N(t) \bullet G'\left(N_{\text{op}}\right). \tag{10}$$

Discretizing equation (10), the following expression can be obtained as follows:

$$\Delta N(t+T) = \Delta N(t) \bullet e^{-G'(N_{\text{op}}) \bullet T} + \frac{1 - e^{-G'(N_{\text{op}}) \bullet T}}{G'\left(N_{\text{op}}\right)} \bullet \Delta Q_{\text{in}}(t), \tag{11}$$

where T is the sampling period.

From equation (11), it is obtained that

$$N(t+T) = N_{op} + \Delta N(t) \bullet e^{-G'(N_{\text{op}}) \bullet T} + \frac{1 - e^{-G'(N_{\text{op}}) \bullet T}}{G'\left(N_{\text{op}}\right)} \bullet \Delta Q_{\text{in}}(t). \tag{12}$$

Furthermore, the time is discretized as $t = k \bullet T$, where $k = 1, 2, 3 \cdots$. Then the accumulation for the $(k+1)$ th sampling period can be obtained as follows:

$$N(k+1) = N_{\text{op}} + \Delta N(k) \bullet e^{-G'(N_{\text{op}}) \bullet T} + \frac{1 - e^{-G'(N_{\text{op}}) \bullet T}}{G'\left(N_{\text{op}}\right)} \bullet \Delta Q_{\text{in}}(k). \tag{13}$$

4.3. Fuzzy Adaptive PID Control Algorithm. In order to guide the traffic demand in the traffic congestion region, it is necessary to obtain the optimal inflow. The traffic congestion region can be regarded as a control object with input and output, and the optimal inflow of the traffic congestion region is the optimal input to the control object, which can be calculated by the control method. Among the control methods, the PID control method has a larger application range and a better stability control effect, but its control parameters are usually determined experimentally or empirically, while the fuzzy control can realize the adjustment of PID control parameters [54, 55]. Based on this, the fuzzy adaptive PID control algorithm is designed to calculate the optimal inflow in the traffic congestion region.

4.3.1. Structure of the Fuzzy Adaptive PID Control Algorithm. The fuzzy adaptive PID control algorithm is based on the PID algorithm. The PID algorithm is divided into an incremental PID algorithm and a positional PID algorithm [56], among which, the incremental PID algorithm can reduce the accumulated error and easily get a better control effect. The adjustment amount of the optimal inflow of the traffic congestion region is calculated by the incremental PID algorithm, and the calculation formula is as follows:

$$\Delta Q_{\text{op}}(k) = k_p(e(k) - e(k-1)) + k_i e(k) + k_d(e(k) - 2e(k-1) + e(k-2)), \tag{14}$$

where $\Delta Q_{\text{op}}(k)$ is the adjustment amount of the optimal inflow at the k th sampling period, k_p, k_i, and k_d are the PID control parameters, $e(k)$ is the deviation between the optimal accumulation and the accumulation at the k th sampling period.

Then the optimal inflow at the k th sampling period can be expressed as follows:

$$Q_{\text{op}}(k) = Q_{\text{op}}(k-1) + \Delta Q_{\text{op}}(k). \tag{15}$$

Based on equations (14) and (15), the fuzzy adaptive PID control algorithm for calculating the optimal inflow is designed, and its structure is shown in Figure 4. The reference value of the fuzzy adaptive PID control algorithm is the optimal accumulation, i.e., N_{op}, and the output is the accumulation, i.e., $N(k+1)$. The control module includes the fuzzy controller, the PID controller, and the traffic flow equilibrium model $F(k)$. The control variable is the adjustment amount of the optimal inflow. In addition, $\Delta e(k)$ in Figure 4 is the change rate of deviation at the k th sampling period, and $F(k)$ is the traffic flow equilibrium model.

4.3.2. Design of the Fuzzy Controller. The fuzzy controller is an important part of the fuzzy adaptive PID control algorithm, which is designed as follows:

(1) Fuzzification of input and defuzzification of output variables

The inputs of the fuzzy controller are the control error $e(k)$ and $\Delta e(k)$, and the outputs are PID parameters change Δk_p, Δk_i, and Δk_d.

Firstly, fuzzy subsets are determined. In this paper, fuzzy states with high control accuracy are selected as the fuzzy subsets of input and output variables, namely {NB, NM, NS, ZO, PS, PM, and PB}, where NB, NM, NS, ZO, PS, PM, and PB, respectively, represent negative big, negative medium, negative small, zero, positive small, positive medium, and positive big.

Secondly, the basic domains of the input and output variables are determined. The basic domains of input variable $e(k)$ and $\Delta e(k)$ are respectively set to $[-0.97N_{\text{op}}, 0.97N_{\text{op}}]$ and $[-0.1N_{\text{op}}, 0.1N_{\text{op}}]$. The basic domains of output variables Δk_p, Δk_i, and Δk_d are, respectively, set to [−24, 24], [−6, 6], and [−10, 10]. The 13 level domain with high control accuracy is chosen as fuzzy domain, which is {−6, −5, −4, −3, −2, −1, 0, 1, 2, 3, 4, 5, 6}.

Finally, the membership function is determined. The steeper the shape of the membership function, the higher the sensitivity, and conversely, the gentler the control characteristic [57]. In this paper, the Gaussian and the triangular membership functions are selected as the membership functions of the input and output variables, respectively.

(2) Determining fuzzy rules

Fuzzy rules need to meet the requirements of the controlled variables and consider the self-adjustment of the PID control parameters. The proportionality factor K_p can speed up the system response and reduce the steady-state error, but an excessive value will produce overshoot and oscillation. The integration factor K_i can eliminate the steady-state error, but an excessive value will cause a large overshoot. The differential factor k_d can attenuate the change of deviation in the control process and enhance the stability of the system.

A total of 49 fuzzy rules of Δk_p, Δk_i, and Δk_d are designed according to the influence of input variables on output variables, as shown in Table 1. Taking the first rule corresponding to the output variable as an example, it can be expressed as: If e is NB and ec is NB then Δk_p is PB, Δk_i is NB and Δk_d is PS. The former expresses the rules, and the conclusion corresponds to the membership functions of the output variables. According to the fuzzy rules, the fuzzy inference engine can get fuzzy outputs. Finally,

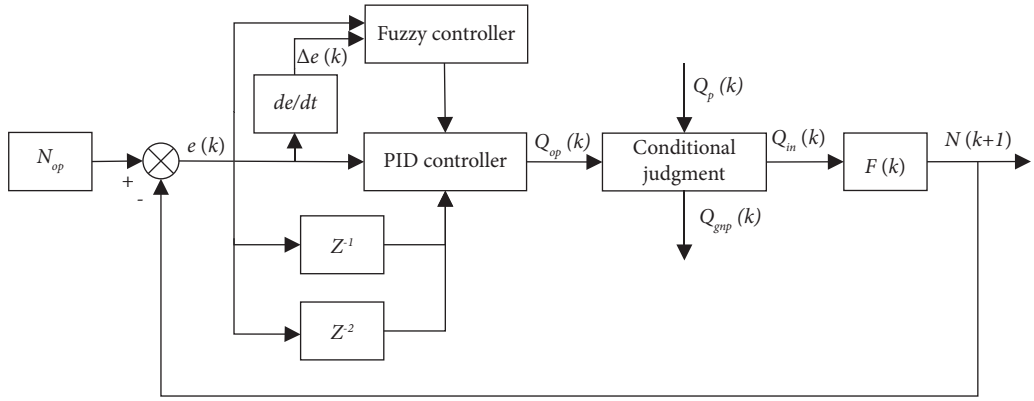

Figure 4: Structure of the fuzzy adaptive PID control algorithm.

the fuzzy outputs are converted to crisp values using defuzzification.

(3) Defuzzification

The centroid method [58] is used for defuzzification in the fuzzy controller. And the adjustment amounts Δk_p, Δk_i, and Δk_d of k_p, k_i, and k_d are obtained. Therefore, the final adjusted values of the PID control parameters are calculated as follows:

$$\begin{cases} k_p = k_{p0} + \Delta k_p, \\ k_i = k_{i0} + \Delta k_i, \\ k_d = k_{d0} + \Delta k_d, \end{cases} \tag{16}$$

where k_{p0}, k_{i0}, and k_{d0} are the initial values of the PID control parameters, which are respectively set to 20, 10, and 1 in this paper.

5. Simulation Experiments

5.1. Example and Simulation Setup. An overly large experimental region has spatial heterogeneity in its internal congestion and needs to be further divided into different subregions. A too small road network cannot show the MFD characteristics of the region well. Therefore, the traffic congestion region contained by Shuangzhu Road, Zhushan Road, Lingshanwan Road, and Xinhua Road in Qingdao, China, is selected as an example to verify the proposed boundary guidance strategy and method. The road network is square, mainly including 41 links and 19 intersections among them are 14 border links and 10 boundary intersections. The road network model is obtained by Vissim according to the actual road network of the example, as shown in Figure 5.

In Figure 5, the blue numbers mark the border links. Detectors (red dots) are placed at the border links to count the amount of inflow and trip completion flow in the example. Additionally, detectors are placed at the upstream and downstream of the links inside the example region to detect vehicle driving speed and delay. The 10 boundary intersections adopt a multiphase fixed signal timing scheme with a cycle length of 150 s, and the internal intersections adopt the cycle length of 120 s or 90 s, according to the actual situation. In addition, the free flow speed is set to 50 km/h.

5.2. Determination of the Optimal Accumulation. To ensure that the example region has a good MFD while being able to simulate the process from free flow to full congestion, we obtained a set of suitable traffic demands after several simulation experiments, which makes the traffic in the region spatially homogeneous. The traffic demand is shown in Table 2. The simulation step is 150 s, and the simulation lasts for 4 hours. The accumulation is calculated by occupancy rate, and the calculation formula can be expressed as follows:

$$N(t) = \sum_{r \in R} \frac{l_r \bullet \eta_r}{l_v} \bullet O_r(t), \tag{17}$$

where r is the internal link, R is the set of links, l_r is the length of the link, η_r is the number of lanes of the link, l_v is the average vehicle length (including headway), and $O_r(t)$ is the time occupation rate of the link r.

According to the simulation, the accumulation and trip completion flows of the example region are obtained and shown as scatter points in Figure 6. Based on the scatter points, the MFD curve is obtained, which also is shown in Figure 6, and its fitting expression is as follows:

$$\begin{aligned} G(N(t)) = {} & -4.975 \times 10^{-8} \times N^3(t) - 1.941 \times 10^{-3} \\ & \times N^2(t) + 8.915 \times N(t). \end{aligned} \tag{18}$$

According to equation (18), the MFD curve reaches its peak when the accumulation is 2124 and the corresponding trip completion flow is 9701 veh/h. Usually, the fluctuation range of traffic control is 1–3% of the optimal accumulation [59]; therefore, the optimal accumulation is set to 2100 vehicles.

5.3. Experimental Results and Analysis. After obtaining the optimal accumulation of the example region, the boundary guidance strategy and method are simulated based on the example region and its traffic demand.

Table 1: Fuzzy control rules for Δk_p, Δk_i, and Δk_d.

$\Delta k_p/\Delta k_i/\Delta k_d$	ec						
	NB	NM		NS	ZO	PS	PM	PB
e	NB	PB/NB/PS	PB/NB/NS	PM/NM/NB	PM/NM/NB	PS/NS/NB	ZO/ZO/NM	ZO/ZO/PS
	NM	PB/NB/PS	PB/NB/NS	PM/NM/NB	PS/NS/NM	PS/NS/NM	ZO/ZO/NS	NS/ZO/ZO
	NS	PMNM/ZO	PM/NM/NS	PM/NS/NM	PS/ZS/NM	ZO/ZO/NS	NS/PS/NS	NS/PS/ZO
	ZO	PM/NM/ZO	PM/NM/NS	PS/NS/NS	ZO/ZO/NS	NS/PS/NS	NM/PM/NS	NM/PM/ZO
	PS	PS/NM/ZO	PS/NS/ZO	ZO/ZO/ZO	NS/PS/ZO	NS/PS/ZO	NM/PM/ZO	NM/PB/ZO
	PM	PS/ZO/PB	ZO/ZO/NS	NS/PS/PS	NM/PS/PS	NM/PM/PS	NM/PB/PS	NB/PB/PB
	PB	ZO/ZO/PB	ZO/ZO/PM	NM/PS/PM	NM/PM/PM	NM/PM/PS	NB/PB/PS	NB/PB/PB

Figure 5: Example regional road network model in VISSIM.

Table 2: Traffic demand of the example region (veh/h).

Border link numbers	Simulation time (s)							
	0–300	300–600	600–1200	1200–1800	1800–3600	3600–5400	5400–7200	7200–14400
1	375	750	1500	2000	3000	4000	4500	5000
2	225	450	900	1200	1800	2400	2700	3000
3	300	600	1200	1600	2400	3200	3600	4000
4	150	300	600	800	1200	1600	1800	2000
5	225	450	900	1200	1800	2400	2700	3000
6	225	450	900	1200	1800	2400	2700	3000
7	225	450	900	1200	1800	2400	2700	3000
8	300	600	1200	1600	2400	3200	3600	4000
9	150	300	600	800	1200	1600	1800	2000
10	300	600	1200	1600	2400	3200	3600	4000
11	300	600	1200	1600	2400	3200	3600	4000
12	150	300	600	800	1200	1600	1800	2000
13	225	450	900	1200	1800	2400	2700	3000
14	225	450	900	1200	1800	2400	2700	3000

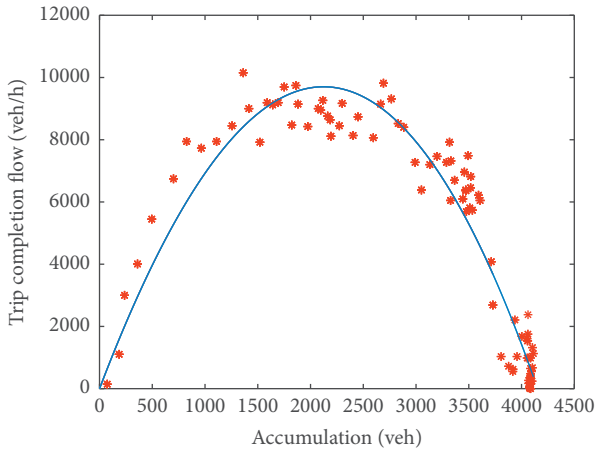

Figure 6: MFD of the example region.

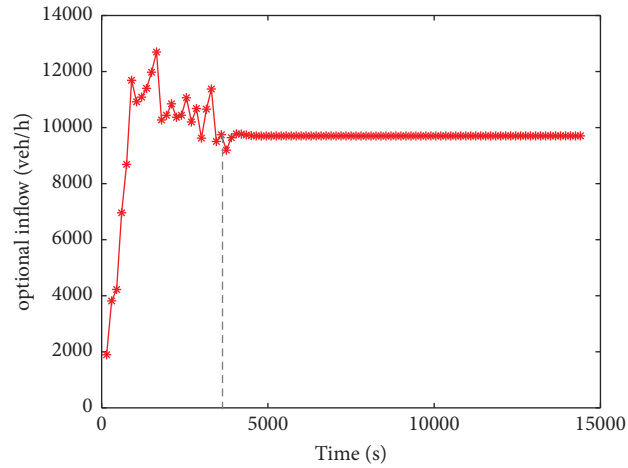

Figure 7: Optimal inflow of the example region.

First, the fuzzy adaptive PID control algorithm is applied to calculate the optimal inflow, and the results are obtained and shown in Figure 7. Before 3600 s, the accumulation is less than the optimal accumulation, and the boundary guidance strategy is not implemented. The inflow in this phase increases rapidly, but with the increase in traffic demand, the accumulation also increases, and the accumulation exceeds the optimal accumulation at about 3600 s. At this point, the fuzzy adaptive PID control algorithm starts to calculate the optimal inflow. And it can be seen from Figure 7 that the optimal inflow gradually stabilizes after small fluctuations.

Thereafter, the simulations of BGS I and BGS II are performed, respectively, according to the optimal inflow. No guidance (NG) as well as perimeter control strategy (PC) are also simulated, where the perimeter control strategy in this paper refers to shutting down the green lights for the entry direction at the boundary intersections when the accumulation exceeds the optimal accumulation and reopening them when the accumulation is lower than the optimal accumulation. The sampling period is 150 s, and the simulation time is 14400 s. Four evaluation indexes of the road network are used, which are the average delay time per vehicle, the average stopped delay per vehicle, the total delay time, and the total travel time. The simulation results are obtained and shown in Table 3. In addition, the inflow, trip completion flow, accumulation, average driving speed, average delay, and average queue delay at border links under different strategies are also obtained, as shown in Figures 8–13, respectively.

As can be seen from Table 3, compared with NG, the four evaluation indexes are reduced under BGS I and BGS II, which proves the feasibility of the two guidance strategies. Furthermore, compared with NG, reductions of the four evaluation indexes under BGS I are 60.2%, 65.7%, 39.9%, and 34.5%, respectively, while under BGS II are 37.4%, 40.5%, 20.6%, and 18.0% respectively. The reductions of the four evaluation indexes under PC are 47.5%, 52.4%, 23.7%, and 19.6% respectively. This indicates that BGS I has a better effect than BGS II and PC. And the reason is that the traffic demand under BGS I with the destinations as the example region is smaller and the inflow is the optimal inflow, while the traffic demand under BGSII is larger and the inflow is greater than the optimal inflow, leading to gradual congestion. PC substantially restricts the vehicles causing congestion on the border links, so its improvement is worse than BGS I. Overall, the boundary guidance strategy has had a good effect on improving the operation state of the road network.

As can be seen from Figure 8, under NG, the inflow of the example region starts to decrease significantly at about 5000 s, and after about 9600 s, only a small inflow is allowed. This is caused by excessive traffic demand, resulting in traffic congestion. Under PC, the frequent restrictive behavior makes the inflow vary drastically. Under BGS I, the inflow can be maintained at about 400 vehicles/step. This shows that BGS I is able to maintain an optimal inflow and avoid congestion. Under BGS II, the inflow is in a small fluctuation after reaching about 400 vehicles/step. Then the inflow decreases significantly at about 10500 s. On the whole, the trend of curve is similar to that under NG, but it maintains a larger inflow for a longer period of time. However, compared to BGS I, it does not maintain a larger inflow all the time. This is due to the excessive traffic demand with the destination as the example region, which is usually related to special events in the example region, such as gathering events.

Figure 9 shows the variation of trip completion flow over time, which is similar to the inflow in Figure 8. Under NG, the trip completion flow starts to decrease significantly after 5000 s. This is also due to the fact that the traffic demand with the destination as the example region is not guided, resulting in congestion. However, under BGS I, the traffic demand is effectively guided so that the trip completion flow does not gradually decrease after a rapid increase in the initial phase but fluctuates near the maximum trip completion. Under PC, the trip completion flow is slightly lower than that under BGS I in general. Compared with NG, BGS II enables the trip completion flow to be maintained near its maximum value for a longer period of time. Then, due to the excessive traffic demand, the trip completion flow gradually decreases, and

Table 3: Results of road network evaluation indexes.

Guidance methods	NG	PC	BGS I	BGS II
Average delay time per vehicle (s)	1716.4	901.1	683.6	1074.1
Average stopped delay per vehicle (s)	1475.8	703.0	505.8	878.1
Total delay time (h)	11978.956	9143.636	7196.888	9505.521
Total travel time (h)	12626.495	10147.86	8267.427	10357.598

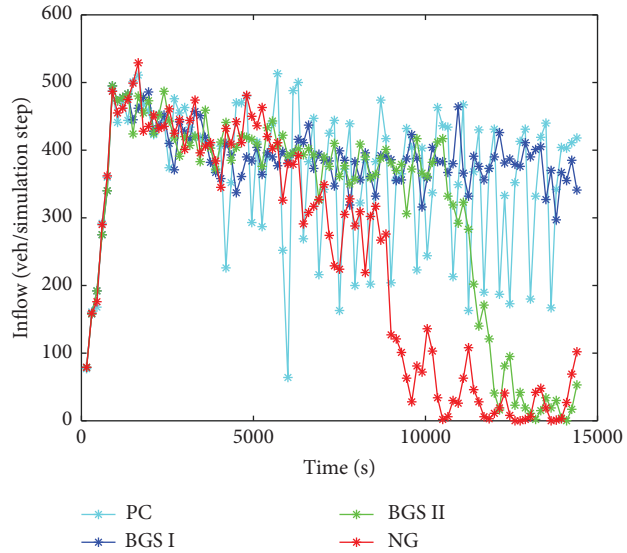

Figure 8: Inflow of the example region under different strategies.

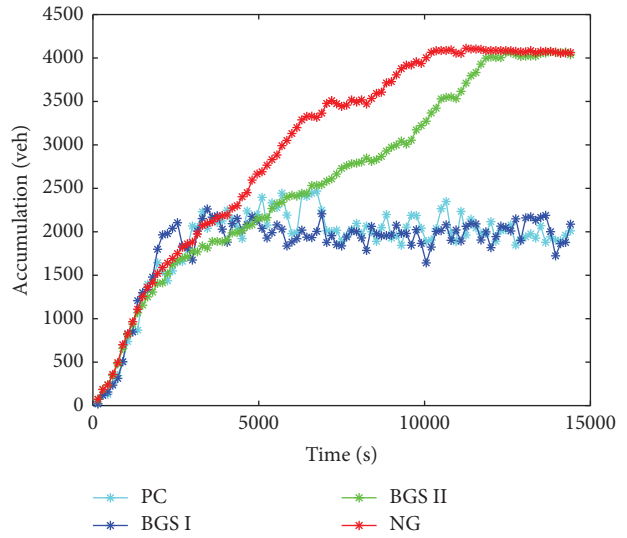

Figure 10: Accumulation of the example region under different strategies.

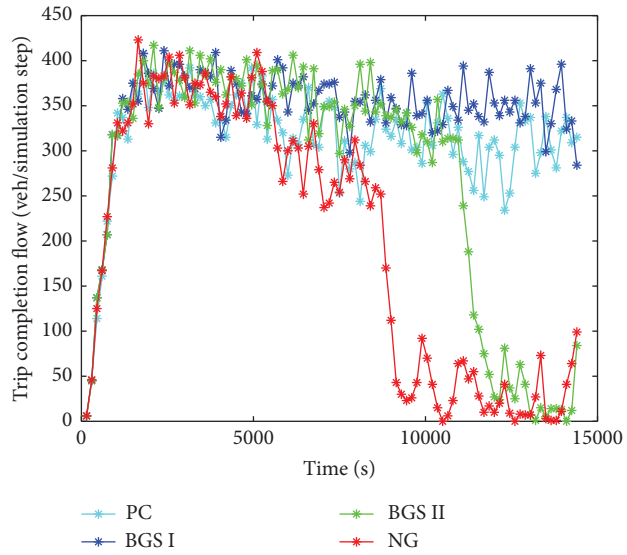

Figure 9: Trip completion flow of the example region under different strategies.

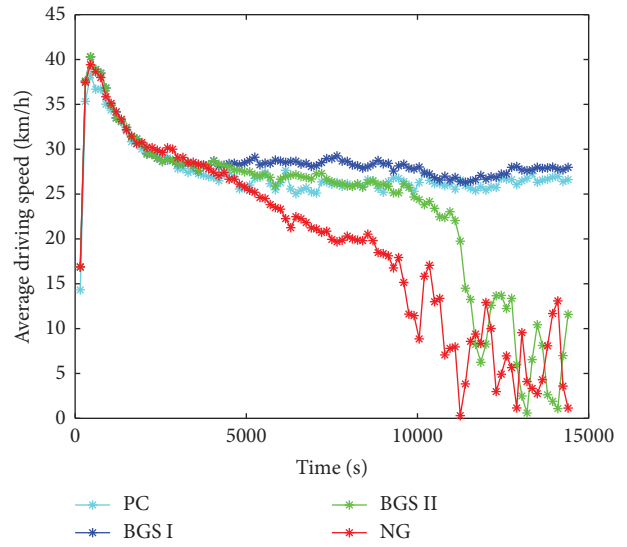

Figure 11: Average driving speed of the example region under different strategies.

finally only a smaller trip completion flow can be maintained. This shows that the boundary guidance strategy can effectively improve the trip completion flow of the example region.

As can be seen from Figure 10, under NG, the accumulation increases in general until it fluctuates slightly near the maximum value at about 10000 s; at this time, the example region is in a fully congested state. Under PC, the restriction on vehicles allows the accumulation to be kept

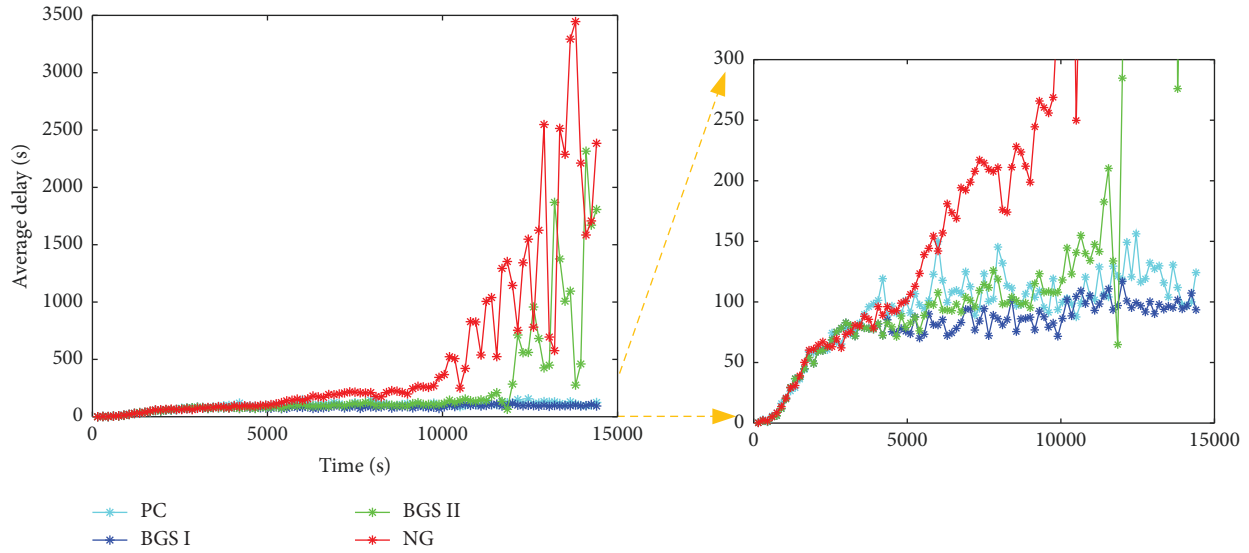

Figure 12: Average delay of the example region under different strategies.

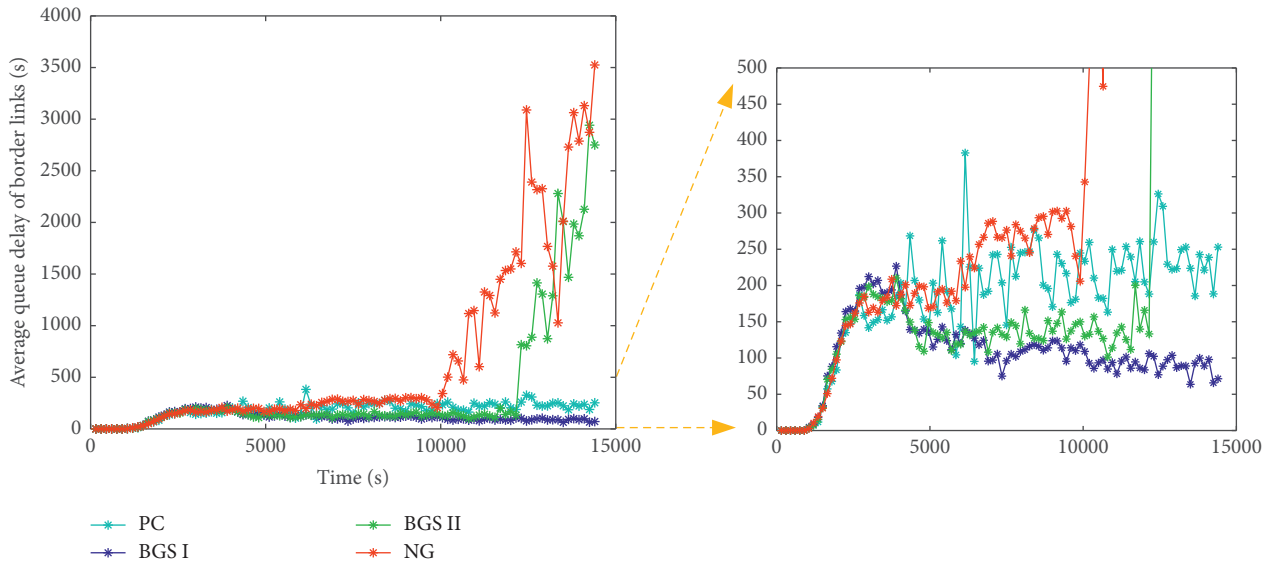

Figure 13: Average queue delay at border links in the example region under different strategies.

near the optimal accumulation. Under BGS I, the accumulation exceeds the optimal accumulation at about 3600 s. Thereafter, the traffic demand is guided so that the accumulation keeps fluctuating slightly near the optimal accumulation. And the goal of guidance is achieved. Under BGS II, the growth rate of accumulation decreases and is in general smaller than the value under NG until it fluctuates slightly around the maximum value after about 12000 s. This indicates BGS II slows down the increase of the accumulation and alleviates the traffic congestion to some extent. However, due to the excessive traffic demand with the destinations as the example region, the trend of gradually increasing accumulation cannot be avoided.

As can be seen from Figure 11, under NG, the average driving speed inside the example region can reach 40 km/h in the initial stage and then gradually decrease until about 10000 s. Thereafter, it fluctuates near a small value, which is due to the large congestion of the road network. Under BGS I, the average driving speed can be maintained at around 28 km/h after a period of decline. Under PC, the average driving speed is slightly lower than that under BGS I in general. Under BGS II, the average driving speed is similar to that under NG and BGS I in the initial stage but gradually shows differentiation at about 3600 s. Compared with BGS I, the average driving speed is lower and decreases rapidly with the gradual increase in time. However, compared with NG, it is generally higher. This shows that the strategy can effectively improve the average driving speed.

As can be seen from Figure 12, under NG, the average delay keeps increasing and then fluctuates significantly, which indicates that traffic congestion gradually worsens. Under BGS I, the average delay can be maintained at about

90 s after about 3600 s. Under PC, the average delay is higher than that under BGS I in general. Under BGS II, the average delay is similar to that under NG, BGS I, and PC until about 3600 s. Compared with BGS I, the average delay is generally higher. However, compared with NG, it is generally smaller. This shows that the strategy is effective in reducing the average delay.

As can be seen from Figure 13, the average queue delay at border links increases consistently and is generally higher than the values under the other strategies. This is due to the overflow of queuing vehicles at the internal intersections caused by excessive traffic congestion within the region, which makes the border links congested. Under PC, the border intersections retain the left-turn and right-turn functions, making the average queue delay lower than the value under NG but higher than the value of BGS I and BGS II until about 12000 s. Under BGS I, the average queue delay is smaller. Under BGS II, the average queue delay increases after 12000 s due to excessive traffic demand with the destination as the example region.

In summary, it can be found that if traffic demand is not guided, the accumulation will increase with the gradual increase in traffic demand until the region is fully congested. This results in the gradual decrease of the inflow, trip completion flow, and average driving speed, while the average delay increases. Although PC can improve the operation state of the road network, it is generally less effective than BGS I and tends to increase the average queue delay at the border links. However, after the implementation of BGS I, the accumulation can be maintained near the optimal accumulation. Thus, the inflow, trip completion flow, and average driving speed are maintained around larger values, as well as the average delay can be reduced. BGS II delays the increase of accumulation. Although inflow, trip completion flow, average driving speed, and average delay are not always maintained in a well range, compared with NG they are all significantly improved. It can be seen that the boundary guidance strategy can improve the operational state of the road network and alleviate traffic congestion.

6. Influence of Connected Vehicle Penetration Rate on the Boundary Guidance Strategy

Although the rapid development of IoVs has made connected vehicles increasingly appear on the road, the presence of more nonconnected vehicles means that the mixed traffic flow of connected and nonconnected vehicles on the road will continue to exist for a long time [60]. Therefore, it is necessary to explore the effectiveness of the use of the boundary guidance strategy under the coexistence of connected and nonconnected vehicles on the road.

BGS I at 20%, 50%, and 80% penetration rates of connected vehicles are simulated, and the results of road network evaluation are obtained, as shown in Table 4. For connected vehicles, they have a 100% compliance rate. And in order to discuss the influence of different penetration rates on the boundary guidance strategy, the simulation results under the full-connected vehicle case (penetration is 100%) as well as the nonconnected vehicle case (penetration rate is 0) are also included in Table 4. In addition, according to Table 4, the improvement of the road network performance under four penetration rates relative to 0 penetration rates is calculated and shown in Figure 14.

As can be seen from Table 4 and Figure 14, compared to the case of nonconnected vehicles, the evaluation results of the road network under different penetration rates are all improved. Especially, under low penetration rates, such as 20%, the average delay is reduced by 27.1%, the average stopped delay per vehicle is reduced by 30.6%, the total delay time is reduced by 12.2%, and the total travel time is reduced by 10.3%. This indicates that BGS I has a good effect even at lower penetration rates. Furthermore, it can be seen that the value of each evaluation index becomes smaller as the penetration rate increases. This indicates that the higher penetration rate, the greater improvement in performance and the better the effect of BGS I on alleviating traffic congestion.

In addition, according to the simulation results under different penetration rates, the inflow, trip completion flow, accumulation, average driving speed, and average delay of the example region are also obtained, as shown in Figure 15. As in Table 4, the results under the case of full-connected and nonconnected vehicles are also added in Figure 15.

As can be seen from Figure 15, the traffic state of the road network is basically similar at the five penetration rates before 3600 s. And after 3600 s, the traffic state shows a difference with the implementation of the boundary guidance strategy. From Figures 15(a) and 15(b), it can be seen that the inflow and trip completion flow begin to decrease significantly at about 6000 s under the case of 0 penetration rate. However, with the gradual increase of the penetration rate, the time at which the inflow and trip completion flow begin to decrease significantly gradually moves backward, reaching about 12600 s at a penetration rate of 80%. When the penetration rate is 100%, the inflow and trip completion flow are maintained near a higher value without any significant decrease. This indicates that BGS I can increase the inflow and trip completion flow under mixed traffic flow, and the guidance effect becomes better with the increase of the penetration rate.

From Figure 15(c), it can be seen that with the increase in the penetration rate, the increasing trend of the accumulation slows down. And when the penetration rate is 100%, the accumulation is maintained near the optimal accumulation. From Figure 15(d), it can be seen that as the penetration rate gradually increases, the time that average driving speed starts to significantly decrease gradually moves later, and the average driving speed can gradually stabilize when the penetration rate is 100%.

As can be seen from Figure 15(e), with the increases of penetration rate, the time when the average delay starts to significantly increase gradually moves later, and when the penetration rate is 100% the average delay is maintained near a lower value. The above shows that with the increase of penetration rate, BGS I becomes more and more effective in reducing the increasing trend of the accumulation, increasing the average driving speed, and reducing the average delay.

Table 4: Results of road network evaluation indexes under five penetration rates.

Penetration rates	0	20%	50%	80%	100%
Average delay time per vehicle (s)	1716.4	1251.5	1115.1	842.3	683.6
Average stopped delay per vehicle (s)	1475.7	1024.0	873.5	640.6	505.8
Total delay time (h)	11978.956	10514.407	10399.378	8673.257	7196.888
Total travel time (h)	12626.495	11324.156	11306.673	9686.979	8267.427

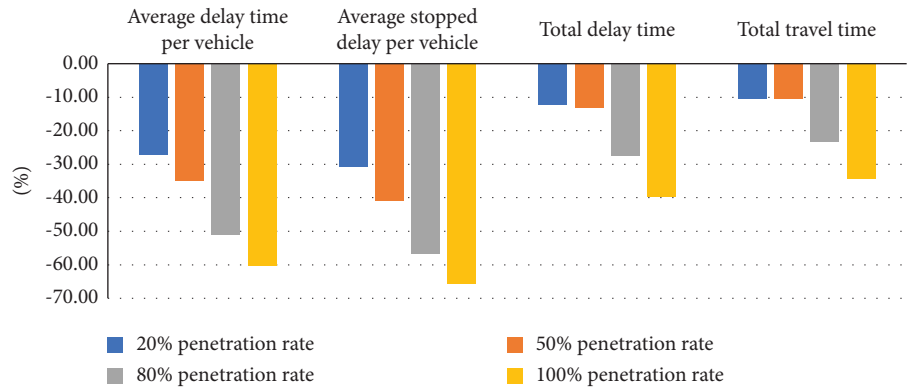

Figure 14: The improvement of the road network performance under four penetration rates.

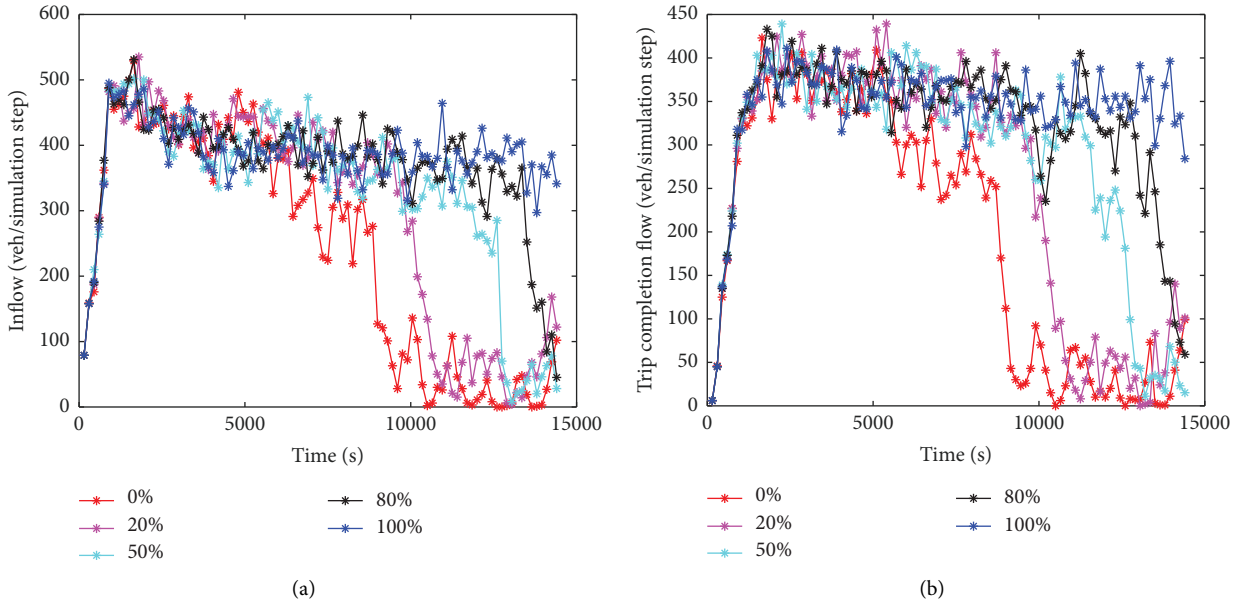

Figure 15: Continued.

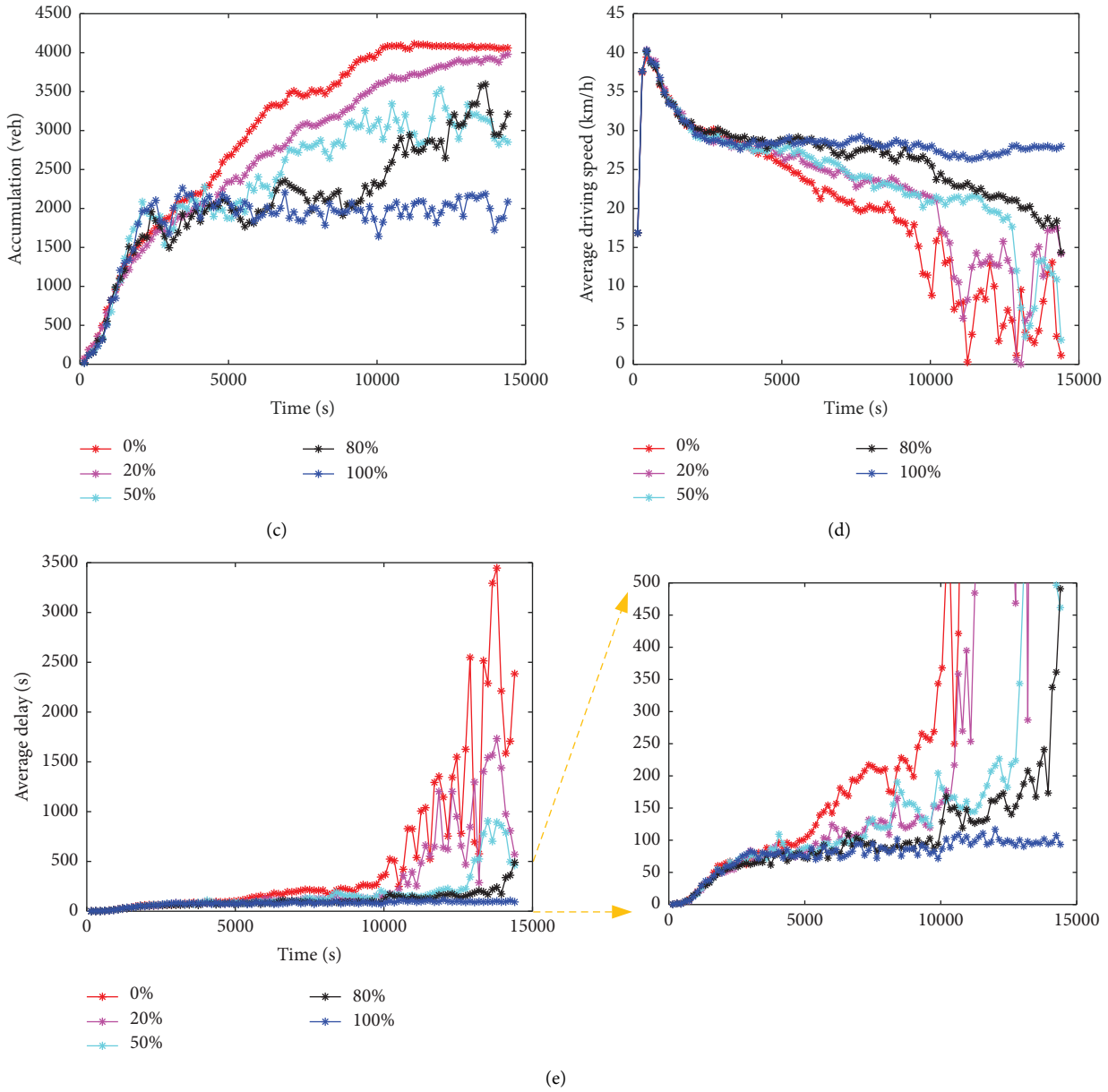

FIGURE 15: Inflow, trip completion flow, accumulation, average driving speed, and average delay of the example region at the five penetration rates. (a) Inflow. (b) Trip completion flow. (c) Accumulation. (d) Average driving speed. (e) Average delay.

In summary, it can be found that the boundary guidance strategy can improve the operation state of the road network in the example region under mixed traffic flow, and the higher the penetration rate, the more significant its effect on alleviating traffic congestion.

7. Conclusion

In this paper, the traffic guidance of urban congestion regions in IoVs environment is studied, and a boundary guidance strategy is proposed. The strategy makes use of the traffic demand information obtained in real time by IoVs to guide the traffic demand according to the destination, so that the operation state of the road network in the traffic congestion region can be improved. The method for the proposed boundary guidance strategy is presented. Firstly, the MFD is used to describe the evolution of the traffic state in the traffic congestion region and determine the optimal accumulation. Then, in order to obtain the real-time accumulation, the traffic flow equilibrium model under the optimal operation state of the traffic congestion region is established and discretized. Finally, a fuzzy adaptive PID control algorithm is designed to calculate the optimal inflow.

Based on an example region, the boundary guidance strategy and method are simulated. The results show that the boundary guidance strategy can maintain optimal accumulation, reduce the increasing trend of the accumulation, improve the trip completion flow, and the average driving speed while reducing the average delay. It is proven that the boundary guidance strategy can effectively improve the

operation state of the road network and alleviate traffic congestion.

Furthermore, the influence of the connected vehicle penetration rate on the boundary guidance strategy is discussed. The boundary guidance strategy is simulated under different penetration rates of connected vehicles. The results show that the boundary guidance strategy is also effective at lower penetration rates. Moreover, with the increase in penetration rate, the boundary guidance strategy becomes more and more effective in reducing the increasing trend of the regional accumulation, increasing the average driving speed, and reducing the average delay.

As mentioned above, a boundary guidance strategy and method for urban traffic congestion regions in IoVs environment are proposed and proven. However, the effectiveness of the boundary guidance strategy is limited in the case when the traffic demand with the destination is too high and the traffic congestion region is too large. At the same time, this paper does not consider the control problem between one congestion region and adjacent congestion regions. For these problems, cooperative control of traffic guidance and signal optimization may be an effective way, which can be further research content. In addition, cooperative guidance among multiple regions under complex traffic environment is also the content of further research.

Data Availability

The data used to support the findings of this study are available from the corresponding author upon request.

Conflicts of Interest

The authors declare that they have no known conflicts of interests.

Authors' Contributions

Chuanxiang Ren contributed to conceptualization, methodology, writing, reviewing, and Editing. Zhen Wang was responsible for conceptualization, methodology, and writing the original draft. Changchang Yin performed supervision, writing, reviewing, and Editing. Hui Xu performed formal analysis. Li Wang contributed to software. Luyao Guo performed investigation. Juntao Li contributed to project administration and funding acquisition.

Acknowledgments

This work is supported by the Key Research and Development Project of Shandong Province (No. 2019GGX101008), National Natural Science Foundation of China (grant no. 72101033) and National Natural Science Foundation of China (grant no. 71831001).

References

[1] Z. Cheng, M. S. Pang, and P. A. Pavlou, "Mitigating traffic congestion: the role of intelligent transportation systems," *Information Systems Research*, vol. 31, no. 3, pp. 653–674, 2020.

[2] E. Angelelli, I. Arsik, V. Morandi, M. Savelsbergh, and M. G. Speranza, "Proactive route guidance to avoid congestion," *Transportation Research Part B: Methodological*, vol. 94, pp. 1–21, 2016.

[3] J. Pan, I. S. Popa, and C. Borcea, "DIVERT: a distributed vehicular traffic re-routing system for congestion avoidance," *IEEE Transactions on Mobile Computing*, vol. 16, no. 1, pp. 58–72, 2017.

[4] X. Tian, C. Liang, and T. Feng, "Dynamic control subarea division based on node importance evaluating," *Mathematical Problems in Engineering*, vol. 2021, Article ID 9923514, 11 pages, 2021.

[5] W. Ackaah, K. Bogenberger, R. L. Bertini, and G. Huber, "Comparative analysis of real-time traffic information for navigation and the variable speed limit system," *IFAC-PapersOnLine*, vol. 49, no. 3, pp. 471–476, 2016.

[6] W. Zhou, M. Yang, M. Lee, and L. Zhang, "Q-learning-based coordinated variable speed limit and hard Shoulder Running control strategy to reduce travel time at freeway corridor," *Transportation Research Record*, vol. 2674, no. 11, pp. 915–925, 2020.

[7] A. Mchergui, T. Moulahi, and S. Nasri, "BaaS: broadcast as a service cross-layer learning-based approach in cloud assisted VANETs," *Computer Networks*, vol. 182, Article ID 107468, 2020.

[8] H. Li and G. Shi, "Design and implementation of vehicle intelligent terminal based on vehicle networking and intelligent technology," in *Proceedings of the 5th International Conference on Mechatronics, Materials, Chemistry and Computer Engineering*, vol. 141, pp. 63–68, Chongqing, China, March 2017.

[9] C. Liu, J. Wang, W. Cai, and Y. Zhang, "An energy-efficient dynamic route optimization algorithm for connected and automated vehicles using velocity-space-time networks," *IEEE Access*, vol. 7, pp. 108866–108877, 2019.

[10] M. K. Alghuson, K. Abdelghany, and A. Hassan, "Telematics-based traffic law enforcement and network management system for connected vehicles," *IEEE Internet of Things Journal*, vol. 8, no. 15, pp. 12384–12397, 2021.

[11] D. A. Mahmood and G. Horváth, "Analysis of the message propagation speed in VANET with disconnected RSUs," *Mathematics*, vol. 8, no. 5, p. 782, 2020.

[12] Z. Yao, L. Shen, R. Liu, Y. Jiang, and X. Yang, "A dynamic predictive traffic signal control framework in a cross-sectional vehicle infrastructure integration environment," *IEEE Transactions on Intelligent Transportation Systems*, vol. 21, no. 4, pp. 1455–1466, 2020.

[13] L. Zhang, Y. Wang, and H. Zhu, "Theory and experiment of cooperative control at multi-intersections in intelligent connected vehicle environment: review and perspectives," *Sustainability*, vol. 14, no. 3, p. 1542, 2022.

[14] J. Jeong, H. Jeong, E. Lee, T. Oh, and D. H. C. Du, "SAINT: self-adaptive interactive navigation tool for cloud-based vehicular traffic optimization," *IEEE Transactions on Vehicular Technology*, vol. 65, no. 6, pp. 4053–4067, 2016.

[15] M. Sommer, S. Tomforde, and J. Haehner, "Forecast-augmented route guidance in urban traffic networks based on infrastructure observations," in *Proceedings of the International Conference on Vehicle Technology and Intelligent Transport Systems*, pp. 177–186, Rome, Italy, January 2016.

[16] Z. Yao, Y. Jiang, B. Zhao, X. Luo, and B. Peng, "A dynamic optimization method for adaptive signal control in

a connected vehicle environment," *Journal of Intelligent Transportation Systems*, vol. 24, no. 2, pp. 184–200, 2020.

[17] S. Zhong, L. Zhou, S. Ma, X. Wang, and N. Jia, "Study on the optimization of VMS location based on drivers' guidance compliance behaviors," *Transport*, vol. 29, no. 2, pp. 154–164, 2014.

[18] Y. Li, M. Tu, and J. Wang, "Layout study of the variable message signs on urban road networks," in *Proceedings of the CICTP 2019: Transportation IN China-Connecting the world*, Nanjing, China, January. 2019.

[19] P. Jindahra and K. Choocharukul, "Short-run route diversion: an empirical investigation into variable message sign design and policy experiments," *IEEE Transactions on Intelligent Transportation Systems*, vol. 14, no. 1, pp. 388–397, 2013.

[20] W. Zhao, M. Quddus, H. Huang, J. Lee, and Z. Ma, "Analyzing drivers' preferences and choices for the content and format of variable message signs (VMS)," *Transportation Research Part C: Emerging Technologies*, vol. 100, pp. 1–14, 2019.

[21] S. AlKheder, F. AlRukaibi, and A. Aiash, "Drivers' response to variable message signs (VMS) in Kuwait," *Cognition, Technology and Work*, vol. 21, no. 3, pp. 457–471, 2019.

[22] W. Zhao, Z. Ma, K. Yang, H. Huang, F. Monsuur, and J. Lee, "Impacts of variable message signs on en-route route choice behavior," *Transportation Research Part A: Policy and Practice*, vol. 139, pp. 335–349, 2020.

[23] J. Shen and G. Yang, "Integrated empirical analysis of the effect of variable message sign on driver route choice behavior," *Journal of Transportation Engineering, Part A: Systems*, vol. 146, no. 2, p. 9, 2020.

[24] J. Roca, P. Tejero, and B. Insa, "Accident ahead? Difficulties of drivers with and without reading impairment recognizing words and pictograms in variable message signs," *Applied Ergonomics*, vol. 67, pp. 83–90, 2018.

[25] P. Tejero, M. Pi-Ruano, and J. Roca, "Better read it to me: benefits of audio versions of variable message signs in drivers with dyslexia," *Annals of Dyslexia*, vol. 70, no. 3, pp. 295–312, 2020.

[26] W. X. Wang, B. H. Wang, W. C. Zheng, C. Y. Yin, and T. Zhou, "Advanced information feedback in intelligent traffic systems," *Physical Review A*, vol. 72, no. 6, Article ID 66702, 2005.

[27] J. Lin, W. Yu, X. Yang, Q. Yang, X. Fu, and W. Zhao, "A real-time en-route route guidance decision scheme for transportation-based cyberphysical systems," *IEEE Transactions on Vehicular Technology*, vol. 66, no. 3, pp. 2551–2566, 2017.

[28] Y. Zhao and H. Zhang, "Research on short-time prediction of dynamical local replanning route guidance method based on HMM," in *Proceedings of the 14th Web Information Systems and Applications Conference*, pp. 19–22, Liuzhou, China, November 2017.

[29] H. Ding, F. Guo, X. Zheng, and W. Zhang, "Traffic guidance–perimeter control coupled method for the congestion in a macro network," *Transportation Research Part C: Emerging Technologies*, vol. 81, pp. 300–316, 2017.

[30] M. Yildirimoglu, I. I. Sirmatel, and N. Geroliminis, "Hierarchical control of heterogeneous large-scale urban road networks via path assignment and regional route guidance," *Transportation Research Part B: Methodological*, vol. 118, pp. 106–123, 2018.

[31] M. Liu, D. Han, D. Li, and M. Wang, "Route guidance during evacuations integrated with perimeter control strategy in large-scale mixed traffic flow networks," *International Journal of Modern Physics C*, vol. 29, no. 11, Article ID 1850112, 2018.

[32] Y. F. Chen, Z. Gao, H. Zhou et al., "Traffic flow guidance algorithm in intelligent transportation systems considering the effect of non-floating vehicle," *Soft Computing*, vol. 23, no. 19, pp. 9097–9110, 2019.

[33] D. Wei and Z. Yang, "Bi-level route guidance method for large-scale urban road networks," *EURASIP Journal on Wireless Communications and Networking*, vol. 2019, p. 127, 2019.

[34] N. Cui, B. Chen, K. Zhang, Y. Zhang, X. Liu, and J. Zhou, "Effects of route guidance strategies on traffic emissions in intelligent transportation systems," *Physica A: Statistical Mechanics and Its Applications*, vol. 513, pp. 32–44, Jan. 2019.

[35] F. Wen, X. Wang, and X. Xu, "Hierarchical Sarsa learning based route guidance algorithm," *Journal of Advanced Transportation*, vol. 2019, Article ID 1019078, 12 pages, 2019.

[36] C. Tang, W. Hu, S. Hu, and M. E. J. Stettler, "Urban traffic route guidance method with high adaptive learning ability under diverse traffic scenarios," *IEEE Transactions on Intelligent Transportation Systems*, vol. 22, no. 5, pp. 2956–2968, 2021.

[37] H. Amer, N. Salman, M. Hawes, M. Chaqfeh, L. Mihaylova, and M. Mayfield, "An improved simulated annealing technique for enhanced mobility in smart cities," *Sensors*, vol. 16, no. 7, p. 1013, 2016.

[38] H. El-Sayed, G. Thandavarayan, and Y. Hawas, "A cost effective route guidance method for urban areas using histograms," *Wireless Communications and Mobile Computing*, vol. 2017, Article ID 4507352, 10 pages, 2017.

[39] K. Lin, C. Li, G. Fortino, and J. J. P. C. Rodrigues, "Vehicle route selection based on game evolution in social internet of vehicles," *IEEE Internet of Things Journal*, vol. 5, no. 4, pp. 2423–2430, 2018.

[40] Z. Y. Sun, Y. Li, W. C. Qu, and Y. Y. Chen, "Collaboration optimization model of dynamic traffic control and guidance based on internet of vehicles," *Modern Physics Letters B*, vol. 32, no. 22, Article ID 1850253, 2018.

[41] C. R. Dow, D. B. Nguyen, S. Cheng, P. Y. Lai, and S. F. Hwang, "VIPER: an adaptive guidance and notification service system in internet of vehicles," *World Wide Web*, vol. 22, no. 4, pp. 1669–1697, 2019.

[42] J. Nie, Z. He, H. Yuan et al., "Automatic route guidance method based on VANETs," in *Proceedings of the 6th International Conference on Information Science and Control Engineering*, pp. 1009–1012, Shanghai, China, December 2019.

[43] Z. Bouyahia, H. Haddad, N. Jabeur, and A. Yasar, "A two-stage road traffic congestion prediction and resource dispatching toward a self-organizing traffic control system," *Personal and Ubiquitous Computing*, vol. 23, no. 5-6, pp. 909–920, 2019.

[44] P. Wang, H. Deng, J. Zhang, and M. Zhang, "Real-time urban regional route planning model for connected vehicles based on V2X communication," *Journal of Transport and Land Use*, vol. 13, no. 1, pp. 517–538, 2020.

[45] Z. Khan, A. Koubaa, and H. Farman, "Smart route: internet-of-vehicles (IoV)-based congestion detection and avoidance (IoV-Based CDA) using rerouting planning," *Applied Sciences*, vol. 10, no. 13, p. 4541, 2020.

[46] L. Zhang, M. Khalgui, and Z. Li, "Predictive intelligent transportation: alleviating traffic congestion in the internet of vehicles," *Sensors*, vol. 21, no. 21, p. 7330, 2021.

[47] T. H. Nguyen and J. J. Jung, "Swarm intelligence-based green optimization framework for sustainable transportation," *Sustainable Cities and Society*, vol. 71, Article ID 102947, 2021.

[48] C. F. Daganzo, V. V. Gayah, and E. J. Gonzales, "Macroscopic relations of urban traffic variables: bifurcations, multivaluedness and instability," *Transportation Research Part B: Methodological*, vol. 45, no. 1, pp. 278–288, 2011.

[49] N. Geroliminis and J. Sun, "Properties of a well-defined macroscopic fundamental diagram for urban traffic," *Transportation Research Part B: Methodological*, vol. 45, no. 3, pp. 605–617, 2011.

[50] E. J. Gonzales, N. Geroliminis, M. J. Cassidy, and C. F. Daganzo, "On the allocation of city space to multiple transport modes," *Transportation Planning and Technology*, vol. 33, no. 8, pp. 643–656, 2010.

[51] Y. Ji, C. Mo, W. Ma, and D. Liao, "Feedback gating control for network based on macroscopic fundamental diagram," *Mathematical Problems in Engineering*, vol. 2016, Article ID 3528952, 11 pages, 2016.

[52] K. Aboudolas and N. Geroliminis, "Perimeter and boundary flow control in multi-reservoir heterogeneous networks," *Transportation Research Part B: Methodological*, vol. 55, pp. 265–281, 2013.

[53] N. Geroliminis, J. Haddad, and M. Ramezani, "Optimal perimeter control for two urban regions with macroscopic fundamental diagrams: a model predictive approach," *IEEE Transactions on Intelligent Transportation Systems*, vol. 14, no. 1, pp. 348–359, 2013.

[54] J. Kluska and T. Żabiński, "PID-like adaptive fuzzy controller design based on absolute stability criterion," *IEEE Transactions on Fuzzy Systems*, vol. 28, no. 3, pp. 523–533, 2020.

[55] N. D. Phu, N. N. Hung, A. Ahmadian, and N. Senu, "A new fuzzy PID control system based on fuzzy PID controller and fuzzy control process," *International Journal of Fuzzy Systems*, vol. 22, no. 7, pp. 2163–2187, 2020.

[56] H. Sang, Y. Zhou, X. Sun, and S. Yang, "Heading tracking control with an adaptive hybrid control for under actuated underwater glider," *ISA Transactions*, vol. 80, pp. 554–563, 2018.

[57] A. Sakalli, T. Kumbasar, and J. M. Mendel, "Towards systematic design of general type-2 fuzzy logic controllers: analysis, interpretation, and tuning," *IEEE Transactions on Fuzzy Systems*, vol. 29, no. 2, pp. 226–239, 2021.

[58] N. K. Arun and B. M. Mohan, "Modeling, stability analysis, and computational aspects of some simplest nonlinear fuzzy two-term controllers derived via center of area/gravity defuzzification," *ISA Transactions*, vol. 70, pp. 16–29, 2017.

[59] X. Yang, J. Chen, M. Yan, Z. He, Z. Qin, and J. Zhao, "Regional boundary control of traffic network based on MFD and FR-PID," *Journal of Advanced Transportation*, vol. 2021, Article ID 9730813, 12 pages, 2021.

[60] D. F. Xie, X. M. Zhao, and Z. He, "Heterogeneous traffic mixing regular and connected vehicles: modeling and stabilization," *IEEE Transactions on Intelligent Transportation Systems*, vol. 20, no. 6, pp. 2060–2071, 2019.